

## The Position, Motion, and Mass of Sgr A\*

Mark J. Reid<sup>\*1</sup>, Karl M. Menten<sup>2</sup>, Reinhard Genzel<sup>3</sup>, Thomas Ott<sup>3</sup>, Rainer Schödel<sup>3</sup>, and Andreas Brunthaler<sup>2</sup>

<sup>1</sup> Harvard-Smithsonian Center for Astrophysics, 60 Garden St., Cambridge, MA 02138, U.S.A.

<sup>2</sup> Max-Planck-Institut für Radioastronomie, Auf dem Hügel 69, D-53121 Bonn, Germany

<sup>3</sup> Max-Planck-Institut für extraterrestrische Physik, Giessenbachstrasse, D-85748 Garching, Germany

Received 3 March 2003

**Key words** Sgr A\*, black holes, proper motions, SiO masers

We report progress on measuring the position of Sgr A\* on infrared images, placing limits on the motion of the central star cluster relative to Sgr A\*, and measuring the proper motion of Sgr A\* itself. The position of Sgr A\* has been determined to within 10 mas on infrared images. To this accuracy, the gravitational source (sensed by stellar orbits) and the radiative source (Sgr A\*) are coincident. Proper motions of four stars measured both in the infrared and radio indicate that the central star cluster moves with Sgr A\* to within  $70 \text{ km s}^{-1}$ . Finally, combining stellar orbital information with an upper limit of  $8 \text{ km s}^{-1}$  for the intrinsic proper motion of Sgr A\* (perpendicular to the Galactic plane), we place a lower limit on the mass of Sgr A\* of  $4 \times 10^5 M_{\odot}$ .

### 1 Introduction

The precise position and proper motion of Sgr A\* are of fundamental importance in order to understand the nature of the super-massive black hole (SMBH) candidate and its environment. Unfortunately, Sgr A\* lies behind about 30 mag of visual extinction, and currently it can only be detected in the radio, infrared, and x-ray bands. While its radio emission is easily detected, the same cannot be said for its infrared and x-ray emission. In both of these wavebands, emissions from nearby (in angle) stars make it difficult to isolate and measure the emission from Sgr A\*. Only with positions accurate to  $\sim 10$  milli-arcseconds (mas) can one confidently separate Sgr A\* from confusing stellar sources and determine its spectral energy distribution and time variations.

Stellar proper motions, accelerations, and even orbits are now being determined to high accuracy at infrared wavelengths, and the position of the central *gravitational* source (presumably Sgr A\*) can be measured to mas accuracy. If Sgr A\* is indeed a SMBH, then the gravitational source, inferred from stellar orbits, and the radiative source, directly seen in the radio band, should coincide to within  $\sim 10$  Schwarzschild radii ( $10R_{sch} \approx 0.08 \text{ mas} \approx 10^{13} \text{ cm}$  for Sgr A\*). Thus measuring the position of Sgr A\* in the infrared to sub-mas levels is of fundamental importance in testing the SMBH paradigm.

The apparent proper motion of Sgr A\* directly determines the sum of the angular rotation speed of the Sun about the Galactic center,  $(\Theta_0 + V_{\odot})/R_0$ , and any peculiar motion of Sgr A\* ( $V_{SgrA*}$ ) with respect to the dynamical center of the Galaxy. Thus, Sgr A\*'s proper motion can provide a direct measurement of Galactic rotation. In addition, the combination of stellar motions and an upper limit on the motion of Sgr A\* itself can yield a strong lower limit to the mass of the SMBH candidate.

This paper reports recent progress on locating Sgr A\* on infrared images, measuring its proper motion, and placing a lower limit on its mass.

\* Corresponding author: e-mail: mreid@cfa.harvard.edu, Phone: +1 617 495 7470, Fax: +1 617 495 7345

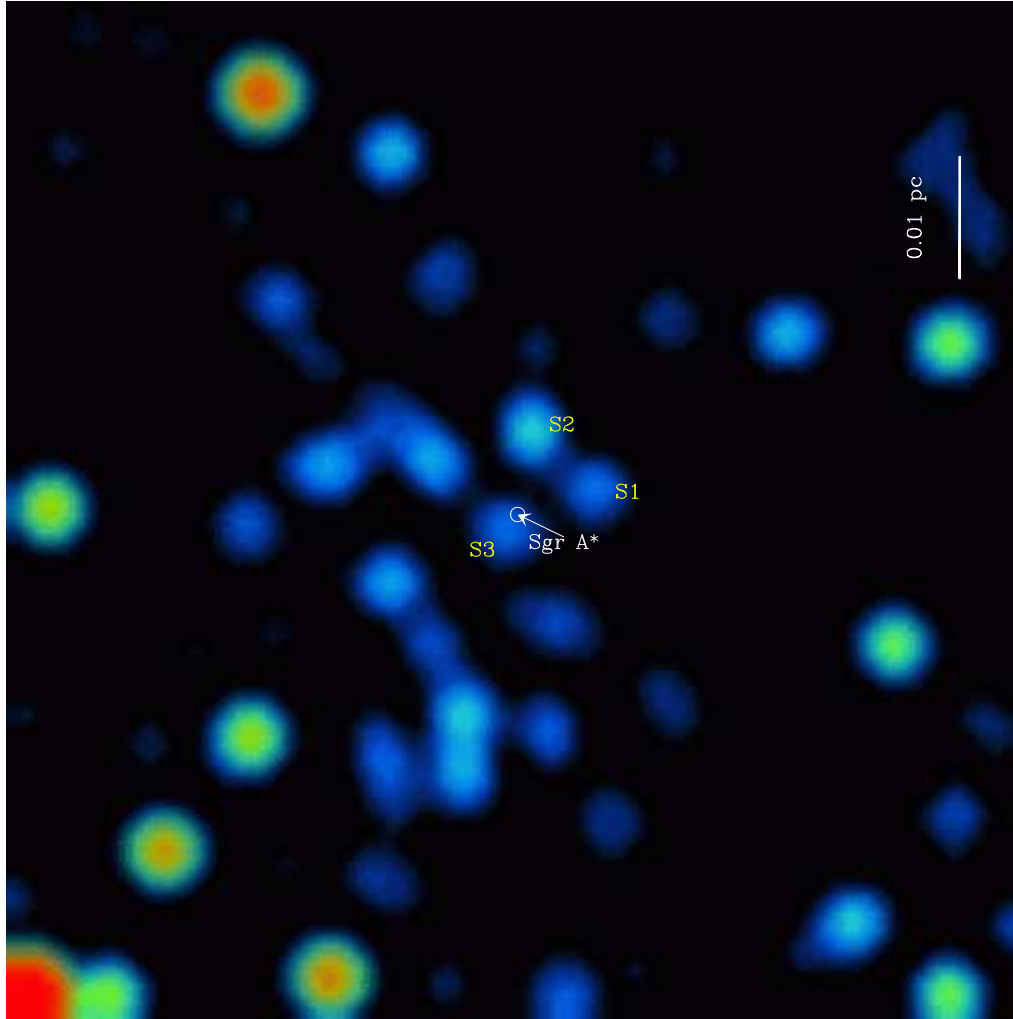


**Fig. 1** Location of Sgr A\* on a July 1995  $2\mu\text{m}$  wavelength image of the inner 2 arcsec of the Galactic center, adapted from Menten et al. (1997) by Reid et al. (2003). The circle centered at the position of Sgr A\* has a radius of 15 mas, corresponding to a  $1\sigma$  position uncertainty.

## 2 Previous Results

Menten et al. (1997) detected SiO maser emission from red giant and supergiant stars within 12 arcsec of Sgr A\*. Since the maser emissions originate from within about five stellar radii of the host star, they can serve to precisely locate the star at radio wavelengths relative to the strong radio source Sgr A\*. Also, the SiO maser stars are very bright at infrared wavelengths, and one can use the radio positions of two or more stars to calibrate the infrared plate scale and rotation and then align the infrared image with the radio image containing Sgr A\*. Following this method, Menten et al. located Sgr A\* on a  $2\mu\text{m}$  wavelength image to an accuracy of 30 mas ( $1\sigma$ ). No source of emission was seen at the position (see Fig. 1) of Sgr A\*, and an upper limit of 9 mJy (de-reddened) was established.

Reid et al. (1999) and Backer & Sramek (1999) published observations of the apparent proper motion of Sgr A\*. Both papers show that Sgr A\* appears to move toward the south-west along the Galactic plane at about  $6\text{ mas yr}^{-1}$ . This is consistent with the angular rotation rate of the Sun in its 220 Myr period about

the Galaxy. Removing the effects of the Sun's orbit yields an upper limit to the peculiar motion of Sgr A\* of about  $20 \text{ km s}^{-1}$ . Reid et al. interpreted this upper limit to indicate that the mass of Sgr A\* exceeds  $\sim 10^3 M_{\odot}$ , ruling out any stellar source.

### 3 Recent Advances

#### 3.1 The Infrared Reference System

Recently, a wide-format infrared camera (CONICA; Lenzen et al. 1998) with an adaptive optics assisted imager (NAOS; Rousset et al. 2000) was installed on one of the ESO 8.2-m VLT telescopes. This has produced excellent data for diffraction-limited imaging. Very deep images of the Galactic center with a field of view of 28 arcsec were taken with these instruments at  $2 \mu\text{m}$  wavelength early in 2002. These images proved to be of excellent quality.

Over the past seven years, radio frequency observations of SiO maser sources in the Galactic center have been conducted with the NRAO VLBA and VLA. Both telescopes have been used to measure positions and proper motions of SiO maser stars with accuracies of about 1 mas and  $1 \text{ mas yr}^{-1}$ , respectively, relative to Sgr A\*. Seven maser stars within 15 arcsec of Sgr A\* have now been measured to these accuracies (Reid et al. 2003). By combining the radio positions of seven maser stars with their apparent positions on the new VLT images, we could determine the infrared plate scales and rotations with high accuracy. After aligning the radio and corrected infrared images, we found the residual differences in the maser star positions to be about 6 mas. This verified that the new infrared images have very small distortions across the field of view and allowed us to determine the position of Sgr A\* with a 10 mas ( $1\sigma$ ) uncertainty (Reid et al. ).

Figure 2 shows a  $2 \mu\text{m}$  wavelength image taken on 2 May 2002, with the position of Sgr A\* and two nearby stars indicated. At this time, the fast moving star S2 was near pericenter in its orbit about Sgr A\* (Schödel et al. 2002). The proximity of S2 to Sgr A\* at this time (16 mas) precludes any significant measurement of the flux density of Sgr A\*. The location for Sgr A\* is within 10 mas of the gravitational source inferred from orbital solutions for the star S2 (Schödel et al. ; Ghez et al. 2003). Thus, the radiative source (Sgr A\*) and the gravitational source of the SMBH candidate are co-located to within about  $1000 R_{Sch}$ .

Previous infrared proper motions have been *relative* motions, with the motion reference defined by setting the average of large numbers of stellar motions to zero. We have compared the radio and infrared proper motions directly in order to transfer the infrared motions to a reference frame tied to Sgr A\* (Reid et al. 2003). In principle, one can make this reference frame transfer using a single star with well determined motions. However, we chose to average the results from the four SiO maser stars within 10 arcsec of Sgr A\* that have measured proper motions both in the radio and infrared. The unweighted mean difference (and standard error of the mean) of these stars is  $0.84 \pm 0.85 \text{ mas yr}^{-1}$  toward the east and  $-0.25 \pm 0.96 \text{ mas yr}^{-1}$  toward the north. Since  $1 \text{ mas yr}^{-1}$  corresponds approximately to  $38 \text{ km s}^{-1}$  (for a distance to the Galactic center of 8.0 kpc), we conclude that the central star cluster moves with Sgr A\* to within about  $40 \text{ km s}^{-1}$  per coordinate axis, or within about  $70 \text{ km s}^{-1}$  for a 3-dimensional motion.

#### 3.2 Proper Motion of Sgr A\*

The *apparent* proper motion of Sgr A\*, with respect to extragalactic radio sources, was measured with the VLBA by Reid et al. (1999). In that program, Sgr A\* was used as a phase reference to calibrate the interferometer phases for two compact radio sources. The location of these sources is shown in Figure 3. Relative to an extragalactic source, Sgr A\* would be expected to move toward the south-west, mostly along the Galactic plane (as depicted in Fig. 3), owing to the orbit of the Sun about the Galactic center.

Figure 4 shows the position residuals of Sgr A\* relative to the compact extragalactic source J1745–283. The positions for 1995 through 1997 are from Reid et al. (1999). Those for 1998 through 2000 are new measurements. As one can see, the apparent motion of Sgr A\* continues along the Galactic plane. The dominant term in the apparent motion of Sgr A\* comes from the orbit of the Sun. This can be decomposed

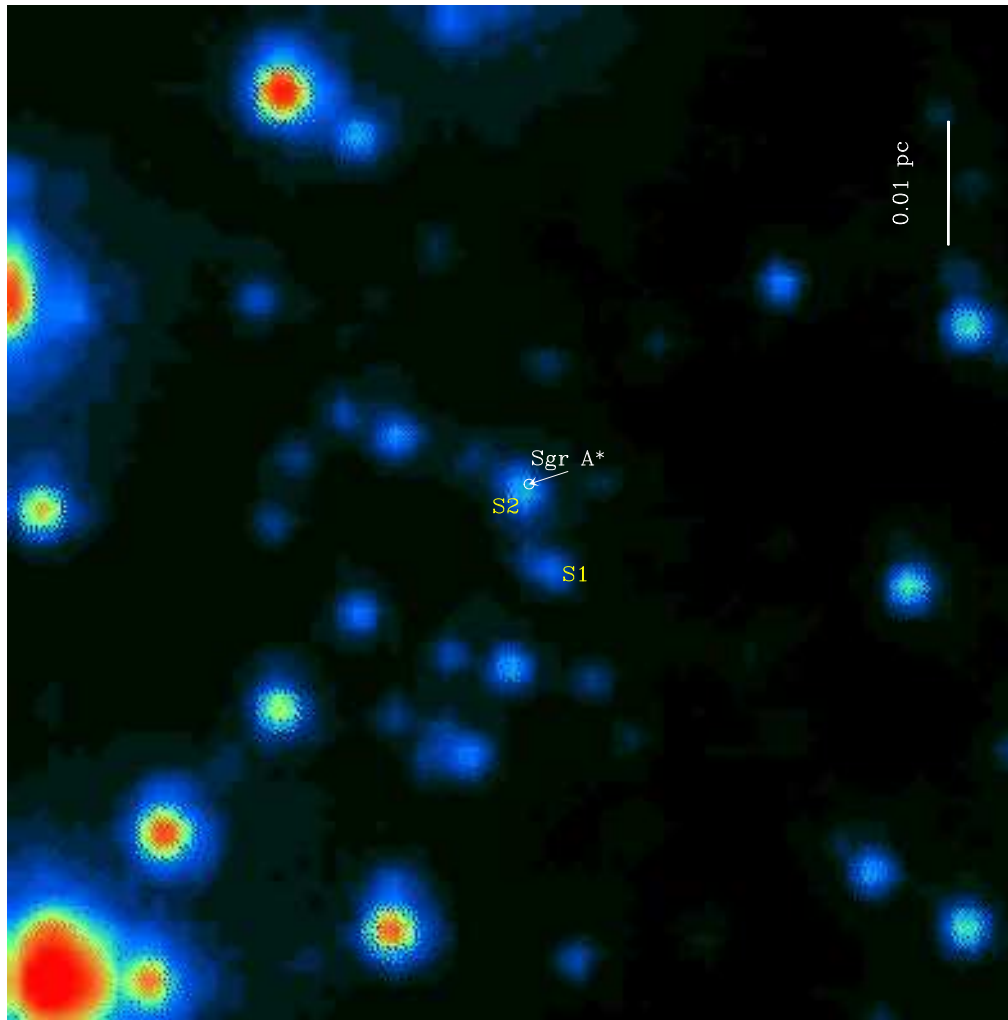


**Fig. 2** Location of Sgr A\* on 2 May 2002 on an infrared ( $2 \mu$ ) image of the inner 2 arcsec of the Galactic center, adapted from Reid et al. (2003). The circle centered at the position of Sgr A\* has a radius of 10 mas, corresponding to a  $1\sigma$  position uncertainty. The star S2 was near pericenter in its orbit about Sgr A\* when this image was taken (Schödel et al 2002; Ghez et al. 2003)

into a circular motion of the local standard of rest,  $\Theta_0/R_0 \approx 220 \text{ km s}^{-1}/8.0 \text{ kpc}$  (see Reid et al. 1999 for details), and the peculiar motion of the Sun,  $V_\odot/R_0 \approx 20 \text{ km s}^{-1}/8.0 \text{ kpc}$ . Removing these terms from the observed proper motion, yields estimates of the peculiar motion of Sgr A\*.

While we currently do not know the component of  $\Theta_0 + V_\odot$  in the plane of the Galaxy to better than about  $10$  to  $20 \text{ km s}^{-1}$ , we do know the component *perpendicular* to the Galactic plane to better than  $1 \text{ km s}^{-1}$ . Since the circular motion of the LSR is, by definition, entirely in the plane of the Galaxy, the only contribution to the apparent motion of Sgr A\* perpendicular to the plane of the Galaxy is the Z-component of the Sun's peculiar motions,  $V_{z_\odot}$ . This component can be estimated by averaging the motions of very large numbers of stars in the Solar neighborhood, which should directly indicate  $-V_{z_\odot}$ . An estimate, using the Hipparcos database, indicates  $V_{z_\odot} = 7.16 \pm 0.38 \text{ km s}^{-1}$  toward the north Galactic pole (Dehnen & Binney 1998). After removing this contribution to the apparent motion of Sgr A\*

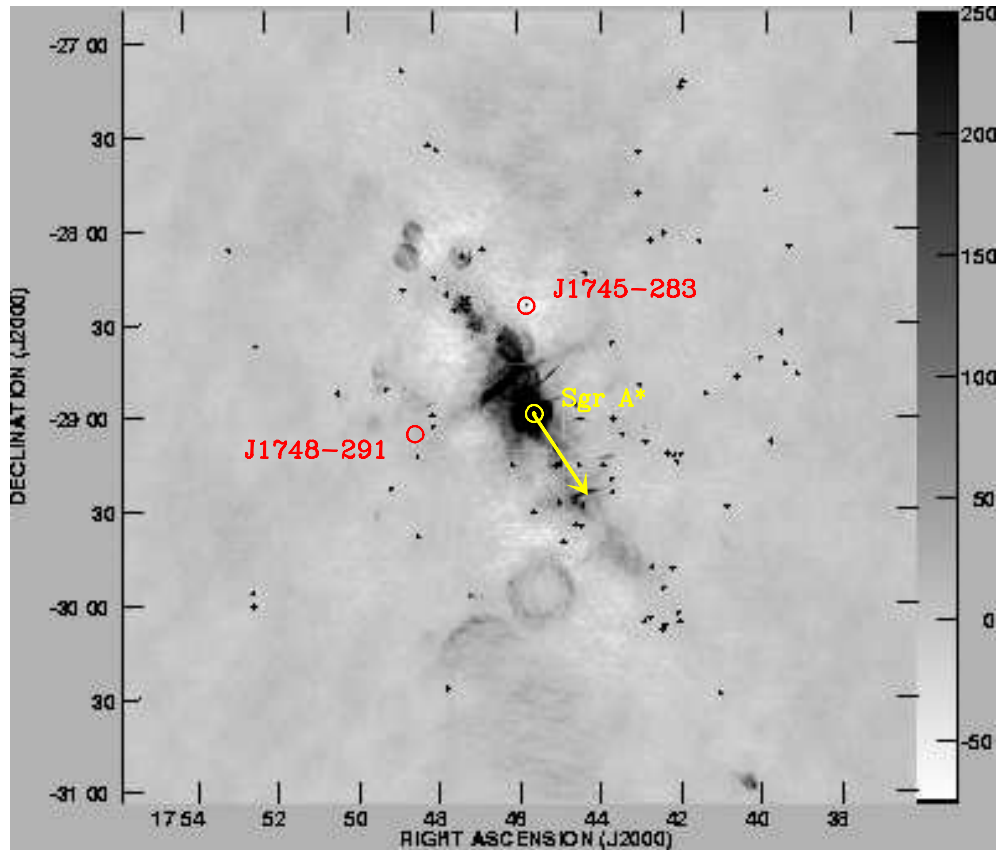


**Fig. 3** Positions of Sgr A\* and two compact extragalactic radio sources superposed on a 90 cm wavelength image of the Galactic center region made with the VLA by LaRosa et al. (2000). The expected motion of Sgr A\*, owing to the orbit of the Sun about the Galactic center, is indicated by the arrow.

perpendicular to the plane of the Galaxy, we arrive at an estimate of  $5 \pm 3 \text{ km s}^{-1}$  for this component of Sgr A\*'s peculiar motion. This result significantly improves on the limits given by Reid et al. (1999) and Backer & Sramek (1999).

#### 4 The Mass of Sgr A\*

From infrared observations of stellar orbits (Schödel et al. 2002, Ghez et al. 2003), we know that a mass of  $\approx 3 \times 10^6 M_{\odot}$  is contained within a radius of  $\approx 100 \text{ AU}$ . With this information, and an upper limit on the Z-component of the velocity of Sgr A\*,  $V_z$ , for which we adopt  $8 \text{ km s}^{-1}$ , one can estimate a lower limit to the mass of Sgr A\*.

The basic parameters of the problem are the total enclosed mass,  $M_{enc}(R)$ , including a possible SMBH and stars with typical individual mass,  $m$ , that are enclosed within a radius,  $R$ , and an upper limit on the Z-component of the velocity,  $V_z$ , of a “test” object (Sgr A\* in our case) of mass  $M$ . In the past, two limiting cases of mass estimators have been discussed for this problem: equipartition of kinetic energy (see Backer

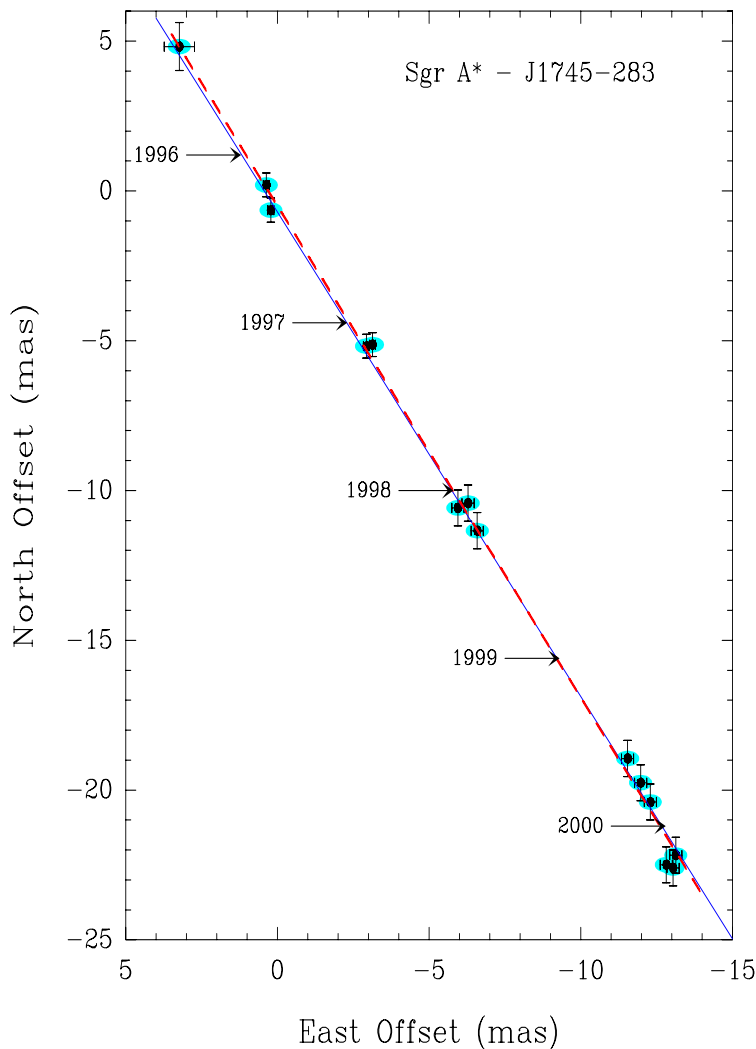


**Fig. 4** Position residuals, with  $1\sigma$  error bars, of Sgr A\* relative to J1745–283 on the plane of the sky. Each measurement is indicated with an ellipse, approximating the apparent scatter broadened size of Sgr A\* at 43 GHz. The dashed line is the variance-weighted best-fit proper motion, and the solid line gives the orientation of the Galactic plane. The expected position of Sgr A\* at the beginning of each calendar year is indicated.

& Sramek 1999) and momentum (see Reid et al. 1999). Equipartition of kinetic energy implies that

$$MV^2 \sim mv^2, \quad (1)$$

where  $v^2 \approx GM_{enc}(R)/R$  is a characteristic stellar velocity at radius  $R$  (which must be great enough so that the mass in stars exceeds that of the test object, i.e.,  $M_{enc}(R) \gtrsim 2M$ ). Equipartition of energy is both theoretically and observationally well founded for the case of stellar clusters. However, for the case of a dominant central mass, which could greatly exceed the total mass of stars (within a given radius), Reid et al. argued that one would be dealing with true orbits and that equipartition of momentum would then be appropriate:

$$MV \sim mv. \quad (2)$$

It turns out that both estimators are correct, but for answering different questions.

If one asks what is the expected velocity of a SMBH that is perturbed by close passages of stars which orbit it, then the momentum equation (2) applies. This is almost surely the case for Sgr A\* and nearby stars such as S1 and S2. For star S2, which has a mass  $m$  of  $\approx 15 M_{\odot}$  (Ghez et al. 2003), during pericenter passage  $v \approx 6500 \text{ km s}^{-1}$  and Eq. (2) implies that one would expect a  $3 \times 10^6 M_{\odot}$  SMBH's peculiar motion to be  $V \sim 0.03 \text{ km s}^{-1}$ . Following this approach one can calculate an extremely conservative lower limit for Sgr A\*'s mass. While this is valid, it is not an optimum estimate.

Alternatively, if we ask for the minimum mass of a central object which does *not* totally dominate the enclosed mass,  $M_{enc}(R)$ , within a given radius  $R$ , and which complies with the observed velocity limit, then we have a different case. For this case, where the enclosed mass in stars within  $R$  is comparable to or exceeds the mass of Sgr A\*,  $M$ , equipartition of kinetic energy should apply. When evaluating Eq. (1) one must use velocities for stars with radii near  $R$ . Conceptually, as the velocity limit for Sgr A\* improves, the estimated mass limit increases quadratically in  $V$ . This continues until the estimated mass dominates over the stellar component and our assumption is violated. At this point, however, one has already ascribed most of the enclosed gravitational mass to Sgr A\*.

A recent paper by Chatterjee, Hernquist & Loeb (2002) analyzes our mass estimation problem in a manner similar to that described above. They assume a black hole at the center of a stellar cluster, which is distributed in space according to a Plummer profile with a characteristic scale  $a$ . The *minimum* black hole mass occurs for  $a$  approximately equal to the radius,  $R$ , within which the enclosed mass is measured. In this case, the mass estimator (their equation 42) can be simplified to the following:

$$M \sim \frac{GM_{enc}(R)m}{V_z^2 R}, \quad (3)$$

provided  $V_z^2 > Gm/R$ , which is met for  $V_z = 8 \text{ km s}^{-1}$ ,  $m = 1 M_{\odot}$ , and  $R = 100 \text{ AU}$ . Then for the observed  $M_{enc}(R) = 3 \times 10^6 M_{\odot}$ , Eq. 3 gives a lower limit to the mass of Sgr A\* of  $M \gtrsim 4 \times 10^5 M_{\odot}$ .

Our lower limit to the mass of Sgr A\* is now within about a factor of 10 of the total mass required by recent IR data. Since the uncertainty in the proper motion ( $\sigma_V$ ) can decrease with the spanned observing time ( $T$ ) as  $\sigma_V \propto T^{-3/2}$ , and the lower limit to the mass of Sgr A\* scales as  $\sigma_V^{-2}$  (until the limit approaches the total enclosed mass), we can expect improvement in the limit for  $M \propto T^3$  over the next few years. When we reach a motion limit of 1 to 2  $\text{km s}^{-1}$  for Sgr A\*, then essentially all of the mass sensed gravitationally by stellar orbits must come from Sgr A\* itself. Should future VLBI measurements at  $\lesssim 1 \text{ mm}$  wavelength show that the intrinsic size of Sgr A\* is  $\lesssim 0.1 \text{ AU}$ , then we may be in a position to conclude that for Sgr A\* most of the mass required for a SMBH is contained within a few  $R_{Sch}$ !

## References

- [1] Backer, D. C. & Sramek, R. A. 1999, ApJ, 524, 805
- [2] Chatterjee, P., Hernquist, L., & Loeb, A. 2002, ApJ, 572, 371
- [3] Dehnen, W. & Binney, J. J. 1998, MNRAS, 387
- [4] Ghez, A. et al. 2003, to appear in ApJ(Lett.)
- [5] LaRosa, T. N., Kassim, N. E., Lazio, T. J. W., & Hyman, S. D. 2000, AJ, 119, 207
- [6] Lenzen, R., Hofmann, R., Bizenberger, P., & Tusche, A. 1998, Proc. SPIE, 3354, 606
- [7] Menten, K. M., Reid, M. J., Eckart, A., & Genzel, R. 1997, ApJ(Lett.), 475, L111
- [8] Reid, M. J., Readhead, A. C. S., Vermeulen, R. C., & Treuhaft, R. N. 1999, ApJ, 524, 816
- [9] Reid, M. J., Menten, K. M., Genzel, R., Ott, T., Schödel, R. & Eckart, A. 2003, to appear in ApJ, 587
- [10] Rousset, G. et al. 2000, Proc. SPIE, 4007, 72
- [11] Schödel, R. et al. 2002, Nature, 419, 694

# Greek symbols – w-greek.sty

$\alpha$	<code>\alpha</code>	$\theta$	<code>\theta</code>	$o$	<code>o</code>	$\tau$	<code>\tau</code>
$\beta$	<code>\beta</code>	$\vartheta$	<code>\vartheta</code>	$\pi$	<code>\pi</code>	$\upsilon$	<code>\upsilon</code>
$\gamma$	<code>\gamma</code>	$\iota$	<code>\iota</code>	$\varpi$	<code>\varpi</code>	$\phi$	<code>\phi</code>
$\delta$	<code>\delta</code>	$\kappa$	<code>\kappa</code>	$\rho$	<code>\rho</code>	$\varphi$	<code>\varphi</code>
$\epsilon$	<code>\epsilon</code>	$\lambda$	<code>\lambda</code>	$\varrho$	<code>\varrho</code>	$\chi$	<code>\chi</code>
$\varepsilon$	<code>\varepsilon</code>	$\mu$	<code>\mu</code>	$\sigma$	<code>\sigma</code>	$\psi$	<code>\psi</code>
$\zeta$	<code>\zeta</code>	$\nu$	<code>\nu</code>	$\varsigma$	<code>\varsigma</code>	$\omega$	<code>\omega</code>
$\eta$	<code>\eta</code>	$\xi$	<code>\xi</code>				
$\Gamma$	<code>\itGamma</code>	$\Lambda$	<code>\itLambda</code>	$\Sigma$	<code>\itSigma</code>	$\Psi$	<code>\itPsi</code>
$\Delta$	<code>\itDelta</code>	$\Xi$	<code>\itXi</code>	$\Upsilon$	<code>\itUpsilon</code>	$\Omega$	<code>\itOmega</code>
$\Theta$	<code>\itTheta</code>	$\Pi$	<code>\itPi</code>	$\Phi$	<code>\itPhi</code>		

Table 1: Slanted greek letters

$\alpha$	<code>\upalpha</code>	$\theta$	<code>\uptheta</code>	$o$	<code>\upo</code>	$\tau$	<code>\uptau</code>
$\beta$	<code>\upbeta</code>	$\vartheta$	<code>\upvartheta</code>	$\pi$	<code>\uppi</code>	$\upsilon$	<code>\upupsilon</code>
$\gamma$	<code>\upgamma</code>	$\iota$	<code>\upiota</code>	$\varpi$	<code>\upvarpi</code>	$\phi$	<code>\upphi</code>
$\delta$	<code>\updelta</code>	$\kappa$	<code>\upkappa</code>	$\rho$	<code>\uprho</code>	$\varphi$	<code>\upvarphi</code>
$\epsilon$	<code>\upepsilon</code>	$\lambda$	<code>\uplambda</code>	$\varrho$	<code>\upvarrho</code>	$\chi$	<code>\upchi</code>
$\varepsilon$	<code>\varepsilon</code>	$\mu$	<code>\upmu</code>	$\sigma$	<code>\upsigma</code>	$\psi$	<code>\uppsi</code>
$\zeta$	<code>\upzeta</code>	$\nu$	<code>\upnu</code>	$\varsigma$	<code>\upvarsigma</code>	$\omega$	<code>\upomega</code>
$\eta$	<code>\upeta</code>	$\xi$	<code>\upxi</code>				
$\Gamma$	<code>\Gamma</code>	$\Lambda$	<code>\Lambda</code>	$\Sigma$	<code>\Sigma</code>	$\Psi$	<code>\Psi</code>
$\Delta$	<code>\Delta</code>	$\Xi$	<code>\Xi</code>	$\Upsilon$	<code>\Upsilon</code>	$\Omega$	<code>\Omega</code>
$\Theta$	<code>\Theta</code>	$\Pi$	<code>\Pi</code>	$\Phi$	<code>\Phi</code>		

Table 2: Upright greek letters



$\alpha$	<code>\bm{\alpha}</code>	$\theta$	<code>\bm{\theta}</code>	$o$	<code>\bm{o}</code>	$\tau$	<code>\bm{\tau}</code>
$\beta$	<code>\bm{\beta}</code>	$\vartheta$	<code>\bm{\vartheta}</code>	$\pi$	<code>\bm{\pi}</code>	$\upsilon$	<code>\bm{\upsilon}</code>
$\gamma$	<code>\bm{\gamma}</code>	$\iota$	<code>\bm{\iota}</code>	$\varpi$	<code>\bm{\varpi}</code>	$\phi$	<code>\bm{\phi}</code>
$\delta$	<code>\bm{\delta}</code>	$\kappa$	<code>\bm{\kappa}</code>	$\rho$	<code>\bm{\rho}</code>	$\varphi$	<code>\bm{\varphi}</code>
$\epsilon$	<code>\bm{\epsilon}</code>	$\lambda$	<code>\bm{\lambda}</code>	$\varrho$	<code>\bm{\varrho}</code>	$\chi$	<code>\bm{\chi}</code>
$\varepsilon$	<code>\bm{\varepsilon}</code>	$\mu$	<code>\bm{\mu}</code>	$\sigma$	<code>\bm{\sigma}</code>	$\psi$	<code>\bm{\psi}</code>
$\zeta$	<code>\bm{\zeta}</code>	$\nu$	<code>\bm{\nu}</code>	$\varsigma$	<code>\bm{\varsigma}</code>	$\omega$	<code>\bm{\omega}</code>
$\eta$	<code>\bm{\eta}</code>	$\xi$	<code>\bm{\xi}</code>				
$\Gamma$	<code>\bm{\itGamma}</code>	$\Lambda$	<code>\bm{\itLambda}</code>	$\Sigma$	<code>\bm{\itSigma}</code>	$\Psi$	<code>\bm{\itPsi}</code>
$\Delta$	<code>\bm{\itDelta}</code>	$\Xi$	<code>\bm{\itXi}</code>	$\Upsilon$	<code>\bm{\itUpsilon}</code>	$\Omega$	<code>\bm{\itOmega}</code>
$\Theta$	<code>\bm{\itTheta}</code>	$\Pi$	<code>\bm{\itPi}</code>	$\Phi$	<code>\bm{\itPhi}</code>		

Table 3: Boldface variants of slanted greek letters

$\alpha$	<code>\pmb{\upalpha}</code>	$\theta$	<code>\pmb{\uptheta}</code>	$o$	<code>\pmb{\upo}</code>	$\tau$	<code>\pmb{\uptau}</code>
$\beta$	<code>\pmb{\upbeta}</code>	$\vartheta$	<code>\pmb{\upvartheta}</code>	$\pi$	<code>\pmb{\uppi}</code>	$\upsilon$	<code>\pmb{\upupsilon}</code>
$\gamma$	<code>\pmb{\upgamma}</code>	$\iota$	<code>\pmb{\upiota}</code>	$\varpi$	<code>\pmb{\upvarpi}</code>	$\phi$	<code>\pmb{\upphi}</code>
$\delta$	<code>\pmb{\updelta}</code>	$\kappa$	<code>\pmb{\upkappa}</code>	$\rho$	<code>\pmb{\uprho}</code>	$\varphi$	<code>\pmb{\upvarphi}</code>
$\epsilon$	<code>\pmb{\upepsilon}</code>	$\lambda$	<code>\pmb{\uplambda}</code>	$\varrho$	<code>\pmb{\varrho}</code>	$\chi$	<code>\pmb{\upchi}</code>
$\varepsilon$	<code>\pmb{\varepsilon}</code>	$\mu$	<code>\pmb{\upmu}</code>	$\sigma$	<code>\pmb{\upsigma}</code>	$\psi$	<code>\pmb{\uppsi}</code>
$\zeta$	<code>\pmb{\upzeta}</code>	$\nu$	<code>\pmb{\upnu}</code>	$\varsigma$	<code>\pmb{\upvarsigma}</code>	$\omega$	<code>\pmb{\upomega}</code>
$\eta$	<code>\pmb{\upeta}</code>	$\xi$	<code>\pmb{\upxi}</code>				
$\Gamma$	<code>\bm{\Gamma}</code>	$\Lambda$	<code>\bm{\Lambda}</code>	$\Sigma$	<code>\bm{\Sigma}</code>	$\Psi$	<code>\bm{\Psi}</code>
$\Delta$	<code>\bm{\Delta}</code>	$\Xi$	<code>\bm{\Xi}</code>	$\Upsilon$	<code>\bm{\Upsilon}</code>	$\Omega$	<code>\bm{\Omega}</code>
$\Theta$	<code>\bm{\Theta}</code>	$\Pi$	<code>\bm{\Pi}</code>	$\Phi$	<code>\bm{\Phi}</code>		

Table 4: Boldface variants of upright greek letters